Long-range vortex domain wall displacement induced by an alternating current: Micromagnetic simulations

Peter Warnicke,[1] Yoshinobu Nakatani,[2] Shinya Kasai,[3] and Teruo Ono[3]
[1]*Department of Engineering Sciences, Uppsala Universitet, 751 21 Uppsala, Sweden*
[2]*University of Electro-communications, Chofu, Tokyo 182-8585, Japan*
[3]*Institute for Chemical Research, Kyoto University, Uji, Kyoto 611-0011, Japan*
(Received 4 April 2008; published 24 July 2008)

A magnetic vortex domain wall, confined in a Permalloy nanowire with periodically varying width, is brought to resonance and long-range motion by means of a spin-polarized alternating current in micromagnetical simulations. The long-range direction of motion is found to be dependent on the vortex chirality but independent of the vortex polarity. Compared to the case where a direct current is used to move the vortex domain wall, the threshold current density for long-range motion is significantly reduced.

DOI: 10.1103/PhysRevB.78.012413 PACS number(s): 75.60.Ch, 85.70.Kh, 75.75.+a

A magnetic domain wall (DW) can serve as a fundamental bit of information in spintronic devices and substantial effort has been focused on manipulating its magnetization in magnetic nanowires using an externally applied field[1–5] or injected spin-polarized current.[6–21] Prospective applications utilizing this concept include memory cells[22] and gates of magnetic logic.[23] Vortex walls (VWs) are of considerable interest because their low stray fields lead to high magnetic stability and low dipolar coupling between neighboring VWs—two factors that open the possibility of high-density integration in storage applications. A current has the advantage of affecting the magnetic structure locally in the absence of externally applied fields. Its driving force is the transfer of spin-angular momentum, from the conduction electrons to the local magnetic structure, by the exchange interaction.[24,25] However, the direct current (dc) required for DW motion is in the order of $10^{11}-10^{12}$ A/m^2.[10,11,26] From an application point of view it is desirable to find ways of reducing this high threshold value.

VW motion induced by alternating current (ac) is an alternative approach that has been predicted to entail a reduced threshold value.[27] Vortex dynamics has been studied in detail.[28–31] The gyroscopic motion of a vortex follows the dynamical equation of Thiele,[31] where the sense of gyration $\mathbf{G}=-2\pi pq\mathbf{e}_z$ along the out-of-plane unit vector $\mathbf{e}_z$ depends on the vortex polarity p and vorticity q. This motion is cyclic about an equilibrium position defined by a pinning site. In order to utilize the properties of a VW, a method for controlled displacement between pinning sites is needed.

Here, we demonstrate a method for displacing a magnetic vortex, trapped in a notched nanowire, in a net direction that is independent of the polarity and instead uniquely determined by the vortex chirality. The motion is based on the resonant behavior of the magnetic microstructure under the influence of a spin-polarized alternating current. Notches along the nanowire serve as pinning sites and restrict the number of equilibrium positions of the vortex.

The current-induced dynamics of the VW is micromagnetically modeled using a computational framework developed by one of the authors.[4] The simulations employ the Landau-Lifshitz-Gilbert equation of motion including adiabatic[32] and nonadiabatic[17,33] spin-transfer effects,

$$\frac{\partial \mathbf{m}}{\partial t} = -\gamma \mathbf{m} \times \mathbf{H} + \alpha \mathbf{m} \times \frac{\partial \mathbf{m}}{\partial t} - u\frac{\partial \mathbf{m}}{\partial x} + \beta u \mathbf{m} \times \frac{\partial \mathbf{m}}{\partial x}, \tag{1}$$

for $4\times 4\times h$ nm^3 cells on a two dimensional grid. The unit vector $\mathbf{m}$ points along the local magnetization, γ is the gyromagnetic ratio, and α is the Gilbert damping parameter. The adiabatic spin torque u has the dimension of velocity and is proportional to the current density J according to $u=-g\mu_B JP/(2eM_s)$, where g is the electron-spin g factor, μ_B the Bohr magneton, P the spin polarization of the current, e the charge of an electron, and M_s the saturation magnetization. The dimensionless parameter $\beta=0.04$ describes the nonadiabaticity of the spin-transfer effect.[17] The effective field $\mathbf{H}$ contains contributions from demagnetization and exchange coupling. The conductive medium is Permalloy for which standard material parameters are used: $M_s=8\times 10^5$ A/m, $\alpha=0.02$, and the exchange coupling constant $A=10^{-11}$ J/m. The applied oscillating current $J=J_0\sin(2\pi ft)$ is flowing along the nanowire with a frequency f and an amplitude J_0. The nanowire is defined with a thickness h in the range of 20–30 nm, width $w=240$ nm, notch wavelength L of 480 nm, and notch depth d between 20 and 80 nm. The geometry is chosen to favor the stability of a VW over other types of DWs.[34]

The long-range propagation direction along the wire depends on the vortex chirality. In Figs. 1(a) and 1(b) the clockwise (CW) and counterclockwise (CCW) chirality are presented, respectively. The VW spans the wire from S_1 to S_2. These two regions along the edges are characterized by spins aligned transverse to the direction of the current flow. Due to the notch geometry, the vortex finds an energetically more favorable position off centered in the x ($-x$) direction for a CW (CCW) chirality. The vortex core (VC) in Fig. 1(a) is 60 nm off centered in the x direction at equilibrium. In Fig. 1(b) an equal offset in the $-x$ direction can be found for the opposite chirality. Asymmetry is also present in the energy barrier for VW propagation, which is lower in the offset direction. In the case of a perfect wire, i.e., a wire with no notches, the VW follows the alternating electron flow and the net vortex displacement remains zero. The situation is the

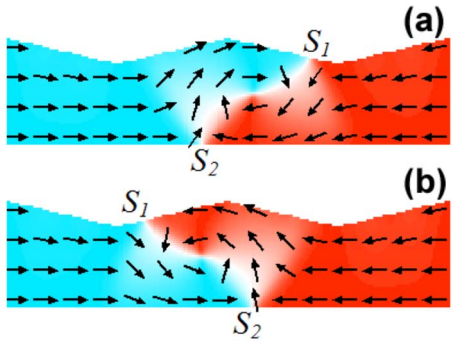

FIG. 1. (Color online) A segment of the wire showing a VW with (a) CW and (b) CCW chirality. The color and arrows indicate the direction of the spins. The wall is spanned from S_1 to S_2, as illustrated by the white region defined by spins aligned transverse to the direction of the current flow.

same for a wire with symmetrical notches on both sides.

The in-plane and out-of-plane angular spin distributions of the initial state can be seen in Figs. 2(a) and 2(b), respectively. As no current is applied, the magnetic structure remains in a state of equilibrium. If a current is applied, the

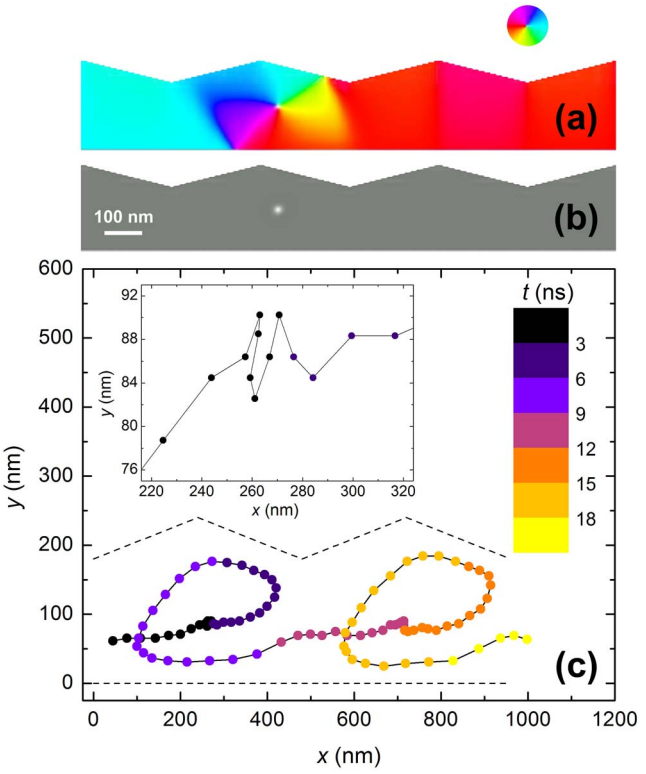

FIG. 2. (Color online) (a) A segment of the nanowire showing the in-plane spin configuration of the initial state. The color-coded circle represents the spin direction in such a way that the configuration is head to head, i.e., spins in the wire are pointing toward the vortex. (b) The corresponding out-of-plane component of the spins reveals the position of the VC. (c) A temporal trajectory of the VC displacement for a 220 MHz signal with $u=80$ m/s where the time interval between two consecutive points is 0.200 ns. The inset shows a closeup of a part of the trajectory. The edges of the nanowire ($d=60$ nm and $h=20$ nm) are represented by the dashed lines.

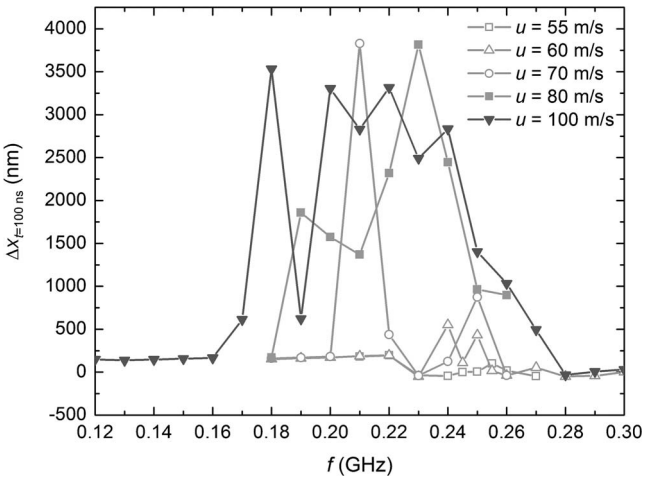

FIG. 3. The frequency dependent VC displacement for a 100 ns ac signal. The critical current density is $J_c=1.3\times10^{12}$ A/m^2, corresponding to $u_c=60$ m/s. The nanowire thickness is 20 nm, the notch depth 80 nm, and the notch wavelength 480 nm.

dynamics can be visualized by separating the motion of the VC from the motion of the VW. The spin torque of an ac pushes the VW in the direction of the electron flow, i.e., back and forth along to the wire. The interplay between (1) the current, (2) the magnetostatic force that tries to restore the equilibrium position, and (3) the gyrotropic nature of the vortex then results in a precessional motion of the VC inside the notch. If the frequency of the ac is tuned to the eigenfrequency of the system, the VW motion is resonantly amplified. For a high enough current density, referred to as the threshold current density J_c, the cyclic motion extends beyond the pinning site and the vortex is absorbed by the neighboring notch. In Fig. 2(c) the time evolution of the VC motion for a continuously applied ac signal with $f=200$ MHz and $u=80$ m/s is shown. The starting point is chosen to illustrate an event where the VW propagates along the nanowire during four current periods. A change in sign of the vortex polarity will reverse the gyrational motion direction of the VC and produce a new trajectory. However, the direction of the net vortex displacement remains the same for both negative and positive polarities.

The graphs in Fig. 3 illustrate the VC displacement of a 100 ns ac signal as a function of frequency for various values of u. At a value below u_c, the VC is removed from equilibrium and enters a steady state of precessional motion at the pinning site. A threshold value of $u_c=60$ m/s, corresponding to $J_c=1.3\times10^{12}$ A/m with $P=0.7$,[35] is required to transfer the VW to the neighboring notch. Sensitivity of frequency decreases with increasing current density. In other words, the bandwidth for long-range propagation increases by one order of magnitude as u is increased from u_c to 100 m/s. In the resonance spectrum, all the graphs show multiple peaks for $u\geq u_c$. For the deeper notches ($d\geq60$ nm), the long-range displacement is always in the positive x direction for a CW chirality. For wires with smaller notch depths ($d\leq40$ nm), the long-range displacement direction is not uniquely determined by the chirality but depends also on the frequency. Using a 100 ns long ac pulse, the CW chirality case with d

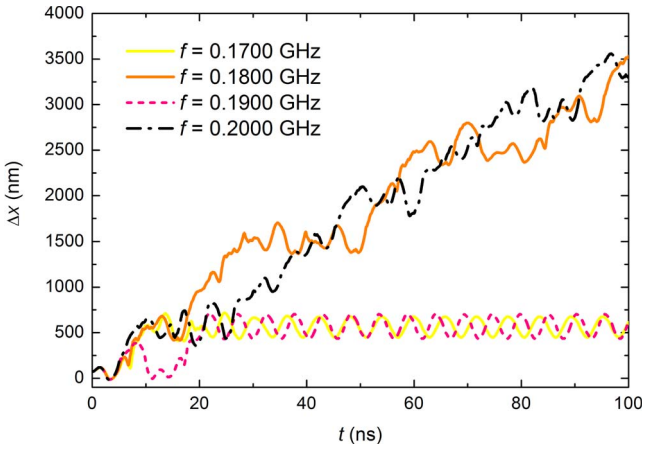

FIG. 4. (Color online) Temporal propagation profile of the VC for different ac frequencies. The current density is 2.1×10^{12} A/m^2, corresponding to $u=100$ m/s. The nanowire thickness is 20 nm, the notch depth 80 nm, and the notch wavelength 480 nm.

$=40$ nm and $u=80$ m/s results in 2.6 μm displacement in the positive x direction for a 170 MHz signal and 3.6 μm in the negative x direction for a 180 MHz signal. This can be understood if we note that the chirality-dependent pinning, and thus the off-centered spatial preference, is less pronounced for these wires.

The time evolution of the VC displacement for different frequencies is shown in Fig. 4. A signal of 0.17 or 0.19 GHz transfers the VW to the neighboring notch, where it enters a steady state of gyrational motion. Signals with frequencies of 0.18 or 0.20 GHz transfer the VW multiple notches. However, the graphs of these signals are characterized by turbulence and passivation of long-range propagation, where a vortex occasionally gets trapped in a notch for multiple current cycles. The same situation is observed for frequencies of 0.21, 0.22, 0.23, and 0.24 GHz (not shown here). The turbulence is attributed to the annihilation of antivortices along the notched edge. An antivortex, nucleated at the wall end S_1, is attracted toward the VC. At a critical point it annihilates with the emission of spin waves. These interact with the VC and slow down its propagation, which can be seen as the wiggle in the inset of Fig. 2(c). One way of suppressing the nucleation of antivortices along the nanowire edges in the field-driven case is to introduce edge roughness.[4]

In order to compare the ac case with the dc case, VW propagation in wires with the same geometry and the same magnetic initial conditions is studied. Equation (1) is used, except that the injected current is now $J=J_0$. The dc electrons are injected in the positive x direction, which, for a CW VW, has a lower energy barrier than the opposite direction. A sufficiently small value of u does not produce any motion of the VW. For a higher value of u, but still smaller than a critical value, the VW is pushed in the direction of the electrons where it enters a state of damped oscillations about a shifted equilibrium position. A value above the critical value will transfer the VW to the next notch. Here, as in the case with alternating current, the critical current density tends to increase with wire thickness. The threshold spin-transfer values for different geometries are seen in Table I. For wires with 60 nm deep notches, u_c is reduced by two-thirds compared to the corresponding dc case.

TABLE I. Critical spin-transfer values u_c for dc and ac under identical initial conditions. The VW is of CW chirality.

d (nm)	h (nm)	dc (u_c) (m/s)	ac (u_c) (m/s)
20	20	120	70
40	20	150	60
60	20	150	50
80	20	140	60
20	25	140	80
40	25	160	80
60	25	160	60
20	30	150	100
80	30	210	150

In conclusion, resonant chirality-dependent long-range displacement of a vortex wall in a notched nanowire can be induced by spin-polarized ac in a frequency interval, which depends on the amplitude of the current. The ac displacement can be triggered at a current density one-third of the value needed for the corresponding dc displacement. This concept opens up the possibility to control nanoscale information based on magnetic domains in nanostructures at reduced currents.

One of the authors thanks the Sweden-Japan Foundation for financial support.

[1] D. Atkinson, D. A. Allwood, G. Xiong, M. D. Cooke, C. C. Faulkner, and R. P. Cowburn, Nat. Mater. **2**, 85 (2003).
[2] G. S. D. Beach, C. Nistor, C. Knutson, M. Tsoi, and J. L. Erskine, Nat. Mater. **4**, 741 (2005).
[3] M. Hayashi, L. Thomas, Y. B. Bazaliy, C. Rettner, R. Moriya, X. Jiang, and S. S. P. Parkin, Phys. Rev. Lett. **96**, 197207 (2006).
[4] Y. Nakatani, A. Thiaville, and J. Miltat, Nat. Mater. **2**, 521 (2003).
[5] T. Ono, H. Miyajima, K. Shigeto, K. Mibu, N. Hosoito, and T. Shinjo, Science **284**, 468 (1999).
[6] E. B. Myers, D. C. Ralph, J. A. Katine, R. N. Louie, and R. A. Buhrman, Science **285**, 867 (1999).
[7] J. A. Katine, F. J. Albert, R. A. Buhrman, E. B. Myers, and D. C. Ralph, Phys. Rev. Lett. **84**, 3149 (2000).
[8] S. Zhang, P. M. Levy, and A. Fert, Phys. Rev. Lett. **88**, 236601 (2002).

[9] J. Grollier, P. Boulenc, V. Cros, A. Hamzic, A. Vaures, A. Fert, and G. Faini, Appl. Phys. Lett. **83**, 509 (2003).
[10] M. Klaui, C. A. F. Vaz, J. A. C. Bland, W. Wernsdorfer, G. Faini, E. Cambril, and L. J. Heyderman, Appl. Phys. Lett. **83**, 105 (2003).
[11] M. Tsoi, R. E. Fontana, and S. S. P. Parkin, Appl. Phys. Lett. **83**, 2617 (2003).
[12] C. K. Lim, T. Devolder, C. Chappert, J. Grollier, V. Cros, A. Vaures, A. Fert, and G. Faini, Appl. Phys. Lett. **84**, 2820 (2004).
[13] E. Saitoh, H. Miyajima, T. Yamaoka, and G. Tatara, Nature (London) **432**, 203 (2004).
[14] G. Tatara and H. Kohno, Phys. Rev. Lett. **92**, 086601 (2004).
[15] N. Vernier, D. A. Allwood, D. Atkinson, M. D. Cooke, and R. P. Cowburn, Europhys. Lett. **65**, 526 (2004).
[16] J. He, Z. Li, and S. Zhang, J. Appl. Phys. **98**, 016108 (2005).
[17] A. Thiaville, Y. Nakatani, J. Miltat, and Y. Suzuki, Europhys. Lett. **69**, 990 (2005).
[18] S. Kasai, Y. Nakatani, K. Kobayashi, H. Kohno, and T. Ono, Phys. Rev. Lett. **97**, 107204 (2006).
[19] A. Himeno, S. Kasai, and T. Ono, Appl. Phys. Lett. **87**, 243108 (2005).
[20] X. Waintal and M. Viret, Europhys. Lett. **65**, 427 (2004).
[21] K. Yamada, S. Kasai, Y. Nakatani, K. Kobayashi, H. Kohno, A. Thiaville, and T. Ono, Nat. Mater. **6**, 270 (2007).
[22] S. S. P. Parkin, U.S. Patent No. 6,834,005 (2004).
[23] D. A. Allwood, G. Xiong, C. C. Faulkner, D. Atkinson, D. Petit, and R. P. Cowburn, Science **309**, 1688 (2005).
[24] L. Berger, Phys. Rev. B **54**, 9353 (1996).
[25] J. C. Slonczewski, J. Magn. Magn. Mater. **159**, L1 (1996).
[26] A. Yamaguchi, T. Ono, S. Nasu, K. Miyake, K. Mibu, and T. Shinjo, Phys. Rev. Lett. **92**, 077205 (2004).
[27] G. Tatara, E. Saitoh, M. Ichimura, and H. Kohno, Appl. Phys. Lett. **86**, 232504 (2005).
[28] R. L. Compton and P. A. Crowell, Phys. Rev. Lett. **97**, 137202 (2006).
[29] K. Y. Guslienko, X. F. Han, D. J. Keavney, R. Divan, and S. D. Bader, Phys. Rev. Lett. **96**, 067205 (2006).
[30] D. L. Huber, Phys. Rev. B **26**, 3758 (1982).
[31] A. A. Thiele, Phys. Rev. Lett. **30**, 230 (1973).
[32] L. Berger, J. Appl. Phys. **71**, 2721 (1992).
[33] S. Zhang and Z. Li, Phys. Rev. Lett. **93**, 127204 (2004).
[34] Y. Nakatani, A. Thiaville, and J. Miltat, J. Magn. Magn. Mater. **290-291**, 750 (2005).
[35] J. Bass and W. P. Pratt, J. Magn. Magn. Mater. **200**, 274 (1999).